

NASA Contractor Report 187543

ICASE Report No. 91-33

ICASE

NUMERICAL RECOVERY OF CERTAIN DISCONTINUOUS ELECTRICAL CONDUCTIVITIES

Kurt Bryan

Contract No. NAS1-18605

March 1991

Institute for Computer Applications in Science and Engineering
NASA Langley Research Center
Hampton, Virginia 23665-5225

Operated by the Universities Space Research Association



National Aeronautics and
Space Administration

Langley Research Center
Hampton, Virginia 23665-5225

(NASA-CR-187543) NUMERICAL RECOVERY OF
CERTAIN DISCONTINUOUS ELECTRICAL
CONDUCTIVITIES Final Report (ICASE) 29 p
CSCL 12A

N91-21800

Unclas

0008366

G3/64

Numerical Recovery of Certain Discontinuous Electrical Conductivities

Kurt Bryan ¹

Institute for Computer Applications in Science and Engineering
NASA Langley Research Center
Hampton, VA 23665

Abstract

The inverse problem of recovering an electrical conductivity of the form $\gamma(x) = 1 + (k-1)\chi_D$ (χ_D is the characteristic function of D) on a region $\Omega \subset \mathbb{R}^2$ from boundary data is considered, where $D \subset \subset \Omega$ and k is some positive constant. A linearization of the forward problem is formed and used in a least squares output method for approximately solving the inverse problem. Convergence results are proved and some numerical results presented.

¹This research was supported by the National Aeronautics and Space Administration under NASA Contract No. NAS1-18605 while the author was in residence at the Institute for Computer Applications in Science and Engineering (ICASE), NASA Langley Research Center, Hampton, VA 23665.

1 Introduction

Impedance tomography seeks to recover information about the internal electrical conductivity of an object by means of voltage and current flux measurements made on its boundary, and so provide a non-invasive, non-destructive imaging technique. The goal of this paper is to provide a method for the approximate recovery of certain types of perturbations of a constant background conductivity. By using methods adapted to the class of conductivities at hand, one hopes to achieve more modest computational loads than more general methods (e.g., [2]) and better continuous dependence of the resulting estimates on the boundary measurements.

The problem may be formulated mathematically as follows. Let Ω be a bounded simply connected open subset of \mathbb{R}^N , $N \geq 2$, with C^2 boundary and D an open subset of Ω with $D \subset\subset \Omega$. Define the function $\gamma(x)$ as

$$\gamma(x) = \begin{cases} 1 & x \in \Omega \setminus D \\ k & x \in D. \end{cases}$$

Let $u(x)$ be the solution to the elliptic boundary value problem

$$\begin{aligned} L_\gamma u &\equiv \nabla \cdot \gamma \nabla u = 0 \quad \text{in } \Omega \\ \partial_\nu u|_{\partial\Omega} &= g \\ \int_{\partial\Omega} u \, dS &= 0, \end{aligned} \tag{1.1}$$

where dS denotes surface measure on $\partial\Omega$, ν is the outward unit normal vector to $\partial\Omega$, $\partial_\nu u = \nu \cdot \nabla u$, and g is a function on $\partial\Omega$ with $\int_{\partial\Omega} g \, dS = 0$. Physically, γ represents the conductivity of the body Ω , g is an applied current flux

density on $\partial\Omega$, and u denotes the electrical potential induced on Ω . It is well known that (1.1) has a unique solution. In this setting the goal of impedance tomography is to recover information about the region D given the value of the potential u on the boundary of Ω induced by the known current flux g . Of course one might apply several different current fluxes, measure the potential that each induces on $\partial\Omega$, and use all of this information to try to recover D . For notational simplicity we will consider only the case of a single boundary measurement, i.e., one applied current flux and measurement of the induced potential on $\partial\Omega$. It is straightforward to extend the results to multiple applied fluxes. The constant k will be considered known *a priori*. Friedman [5] has proven results regarding the detection and identification of the region D from a single boundary measurement and some results concerning the continuous dependence of D on the boundary data also exist (see [3]). It is known that D is uniquely determined if one takes all possible boundary measurements, that is, if one applies all possible currents fluxes and measures the induced voltages for each (see [7] or [8]).

It will be necessary to restrict the domains D to lie in a certain admissible class. It will be assumed that this class is described by a finite number of parameters, so that $D = D(q)$ with $q \in Q$, where Q is a compact subset of \mathbb{R}^m . Certain restrictions on the map $q \rightarrow D(q)$ will be made later.

We use $W^k(\Omega)$ to denote the Sobolev space obtained by completing $C^\infty(\bar{\Omega})$ with respect to the norm

$$\|\phi\|_{W^k(\Omega)} = \sum_{|\alpha| \leq k} \|\partial^\alpha \phi\|_{L^2(\Omega)}.$$

The solution to (1.1) lies in $W^1(\Omega)$ (see [6]) for sufficiently regular g .

In practice one does not measure the potential at every point on $\partial\Omega$, but only at finitely many locations. We will thus specify an observation mechanism for the potential on $\partial\Omega$. Let N_i , $i = 1, \dots, M$, be open subsets of $\partial\Omega$. For each N_i let $f_i(x)$ be a bounded measurable function supported in N_i . We will then assume that the measurement of the potential on $\partial\Omega$ is of the form $y = \mathcal{F}(u)$ where the map $\mathcal{F} : L^2(\partial\Omega) \rightarrow \mathbb{R}^M$ is defined by

$$\mathcal{F}_i(\phi) = \int_{N_i} f_i \phi \, dS,$$

$i = 1, \dots, M$. Note that the restriction of a function in $W^1(\Omega)$ to $\partial\Omega$ makes sense as an element of $L^2(\partial\Omega)$ so that the integral is defined and finite if $\phi \in W^1(\Omega)$. Since the trace operator is continuous from $W^1(\Omega)$ to $L^2(\partial\Omega)$, the operator \mathcal{F} is continuous from $W^1(\Omega)$ to \mathbb{R}^m .

One method for approaching the inverse problem is to use an output least squares method. Specifically, let d_i denote the potential observed by the electrode at N_i for some unknown region $D(q_0)$ when the current flux g is applied and let $y^q = \mathcal{F}(u^q)$ where u^q solves (1.1) with $D = D(q)$. Define a fit-to-data function $J(q)$ by

$$J(q) = \frac{1}{2} \sum_{i=1}^M |y_i^q - d_i|^2.$$

One may then attempt to solve the inverse problem by seeking a solution to the optimization problem of finding $q^* \in Q$ which minimizes $J(q)$. One of the drawbacks of this approach is that every evaluation of $J(q)$ requires one to solve the forward problem (1.1), which may be costly computationally. Also, one has no (obvious) direct way to compute the derivatives of $J(q)$ with respect to q ; availability of these derivatives is helpful in any optimization

problem. We will instead consider a modification of the inverse problem, replacing the solution \tilde{u} of (1.1) by \tilde{u} , its tangent line approximation in the k variable about the point $k = 1$. The function \tilde{u} may be computed explicitly, much more quickly than u , and using \tilde{u} in place of u in the definition of J allows us to compute directly the derivatives of J with respect to the parameter q , provided the map $q \rightarrow D(q)$ is suitably restricted.

The organization of the paper is as follows. The second section deals with preliminary results concerning the Neumann function for the Laplacian on a bounded region. The third section establishes the differentiability of the map $k \rightarrow u(x)$ for $x \in \partial\Omega$ for u solving (1.1) and the accuracy of the linearization about $k = 1$. The original inverse problem is replaced by an inverse problem involving the linearized solution \tilde{u} . In the fourth section a computational method for solving the linearized version of the inverse problem is presented and convergence results are proved. The final section contains numerical results; the algorithm for solving the linearized inverse problem is applied to boundary data generated by solving the linearized forward problem (for \tilde{u}) and the original equations (1.1).

2 The Neumann Function

The *Neumann* function for the Laplacian on Ω is a function $N(x, \xi)$ defined on $\Omega \times \Omega$ which satisfies, for each $x \in \Omega$, the conditions

$$\begin{aligned}\Delta_{\xi} N(x, \xi) &= -\delta_x \\ \partial_{\nu_{\xi}} N(x, \xi)|_{\xi \in \partial\Omega} &= \frac{-1}{|\partial\Omega|}\end{aligned}$$

with the normalization $\int_{\partial\Omega} N(x, \xi) dS_\xi = 0$. Here δ_x denotes the delta function at x and Δ_ξ is the Laplacian applied in the ξ variable. For $\Omega \subset \subset \mathbb{R}^2$ one can verify that the Neumann function is given by

$$N(x, \xi) = \Gamma(|x - \xi|) + \sigma(x, \xi)$$

where $\Gamma(r) = -\frac{1}{2\pi} \log(r)$ and σ is chosen to solve

$$\begin{aligned} \Delta_\xi \sigma(x, \xi) &= 0 \\ \partial_{\nu_\xi} \sigma(x, \xi)|_{\xi \in \partial\Omega} &= -\frac{1}{|\partial\Omega|} - \partial_{\nu_\xi} \Gamma(x, \xi)|_{\xi \in \partial\Omega} \\ \int_{\partial\Omega} \sigma(x, \xi) dS_\xi &= 0. \end{aligned}$$

Also, if $u_0 \in C^2(\bar{\Omega})$ satisfies

$$\begin{aligned} \Delta u_0 &= f \\ \partial_\nu u_0|_{\partial\Omega} &= g \\ \int_{\partial\Omega} u_0 dS &= 0 \end{aligned}$$

then u_0 can be represented as

$$u_0(x) = \int_{\partial\Omega} N(x, \xi) g(\xi) dS_\xi - \int_\Omega N(x, \xi) f(\xi) d\xi \quad (2.1)$$

for each $x \in \Omega$.

The remainder of the paper will be limited to the case in which $\Omega \subset \mathbb{R}^2$ and we shall next make a restriction which, for simply connected Ω , represents no loss of generality. Specifically, we assume that Ω is the unit disk, for one can always map the region Ω to the unit disk conformally via a mapping ϕ . It is straightforward to verify that the function $u \circ \phi^{-1}$ defined on the

disk satisfies an equation of the form (1.1) with the same constant k and D replaced by $\phi(D)$. The conformal map ϕ also maps the unit normal vector field on $\partial\Omega$ to a normal (though not unit) vector field on the boundary of the disk, so that the transformed problem has Neumann data at the boundary. In the case in which Ω is the unit disk one can verify that the Neumann function is given by

$$N(x, \xi) = -\frac{1}{2\pi}(\log(|x - \xi|) + \log(|\bar{x} - \xi|))$$

where $\bar{x} = x/|x|^2$.

3 A Linearization

For a particular region D in Ω and fixed Neumann data g , let $u(k, x)$ denote the parameter-dependent solution to (1.1). Let $u_0(x)$ denote the harmonic function on Ω defined by (2.1) and define

$$\psi(x) = -\int_{\partial D} u_0(\xi) \partial_{\nu_\xi} N(x, \xi) dS_\xi$$

for $x \in \partial\Omega$.

Lemma 3.1 *For fixed $x \in \partial\Omega$ the map $k \rightarrow u(k, x)$ is differentiable with respect to k at $k = 1$, and its derivative is given by $\psi(x)$.*

Actually, we will show something a bit stronger, namely that

$$\lim_{k \rightarrow 1} |u(k, x) - u_0(x) - (k - 1)\psi(x)| \leq C(k - 1)^2$$

for some constant C , so that the error in the tangent line approximation is $O((k-1)^2)$.

Before proving Lemma 3.1 we will need a couple of facts about the function u solving (1.1). It is shown in [9], section 16 ("Diffraction Problems") that $u \in W^2(\Omega \setminus D)$ and $u \in W^2(D)$. It is also shown that the function u is continuous across ∂D and satisfies the jump condition $\partial_\nu^\epsilon u = k \partial_\nu^i u$ on ∂D , where $\partial_\nu^i u$ denotes the outward unit normal derivative of u on ∂D as measured from inside D , and $\partial_\nu^\epsilon u$ is the outward unit normal derivative as measured from $\Omega \setminus D$. Using these facts one can prove the following proposition.

Proposition 3.1 *For $x \in \bar{\Omega} \setminus D$ the solution u to equation (1.1) satisfies*

$$u(k, x) = u_0(x) + (1 - k) \int_{\partial D} u(k, \xi) \partial_{\nu_\xi} N(x, \xi) dS_\xi. \quad (3.1)$$

For $x \in \partial D$, u satisfies the integral equation

$$u(k, x) = \frac{2(1 - k)}{1 + k} \int_{\partial D} u(k, \xi) \partial_{\nu_\xi} N(x, \xi) dS_\xi + \frac{2}{1 + k} u_0(x). \quad (3.2)$$

Proof: Since k is fixed throughout the proof, we'll simply write $u(x)$ for the function u . To prove equation (3.1), take $x \in \bar{\Omega} \setminus D$ and $B_\epsilon(x)$ a ball of radius ϵ around x . Applying the divergence theorem on $\Omega \setminus (D \cup B_\epsilon(x))$ (valid since u is W^2 on this region) and using the fact that $u(\xi)$ and $N(x, \xi)$ are harmonic as functions of ξ on this region shows that

$$\begin{aligned} 0 &= \int_{\partial \Omega} (u(\xi) \partial_{\nu_\xi} N(x, \xi) - N(x, \xi) \partial_\nu u(\xi)) dS_\xi \\ &\quad - \int_{\partial B_\epsilon(x)} (u(\xi) \partial_{\nu_\xi} N(x, \xi) - N(x, \xi) \partial_\nu u(\xi)) dS_\xi \\ &\quad - \int_{\partial D} (u(\xi) \partial_{\nu_\xi}^\epsilon N(x, \xi) - N(x, \xi) \partial_\nu^\epsilon u(\xi)) dS_\xi, \end{aligned}$$

where the vector field ν of the boundary of $B_\epsilon(x)$ points away from the ball. Using the properties of the Neumann function and the representation formula (2.1) yields

$$\begin{aligned} 0 = -u_0(x) & - \int_{\partial B_\epsilon(x)} (u(\xi) \partial_{\nu_\xi} N(x, \xi) - N(x, \xi) \partial_\nu u(\xi)) dS_\xi \\ & - \int_{\partial D} (u(\xi) \partial_{\nu_\xi}^\epsilon N(x, \xi) - N(x, \xi) \partial_\nu^\epsilon u(\xi)) dS_\xi. \end{aligned}$$

As ϵ goes to zero standard potential theory arguments (e.g., [4], chapter 3) give

$$0 = -u_0(x) + u(x) - \int_{\partial D} (u(\xi) \partial_{\nu_\xi}^\epsilon N(x, \xi) - N(x, \xi) \partial_\nu^\epsilon u(\xi)) dS_\xi. \quad (3.3)$$

Note if $x \in \partial\Omega$ then $B_\epsilon(x)$ is only “half” of a disk, although in this case $N(x, \xi) = 2\Gamma(x, \xi)$, so that (3.3) remains valid. Finally, since N is smooth near ∂D as a function of ξ , $\partial_{\nu_\xi}^\epsilon N = \partial_{\nu_\xi}^i N$ so that

$$\begin{aligned} \int_{\partial D} N(x, \xi) \partial_\nu^\epsilon u(\xi) dS_\xi &= k \int_{\partial D} N(x, \xi) \partial_\nu^i u(\xi) dS_\xi \\ &= k \int_{\partial D} \partial_{\nu_\xi} N(x, \xi) u(\xi) dS_\xi \end{aligned}$$

where the last equality follows by applying the divergence theorem on D . When substituted into equation (3.3), the last equality yields (3.1).

To prove equation (3.2), rewrite the integral in equation (3.1) as

$$\begin{aligned} \int_{\partial D} u(\xi) \partial_{\nu_\xi} N(x, \xi) dS_\xi &= \int_{\partial D} \partial_{\nu_\xi}^i u(\xi) N(x, \xi) dS_\xi \\ &= \frac{1}{k} \int_{\partial D} \partial_\nu^\epsilon u(\xi) N(x, \xi) dS_\xi. \end{aligned}$$

When this is combined with equation (3.1), we obtain, for $x \in \bar{\Omega} \setminus D$,

$$u(x) = u_0(x) + \frac{1-k}{k} \int_{\partial D} \partial_\nu^\epsilon u(\xi) N(x, \xi) dS_\xi. \quad (3.4)$$

This expression remains valid for $x \in \partial D$ as well, since the singularity in the integrand is only logarithmic and u is continuous across ∂D . For $x \in \partial D$ let $D_\epsilon = D \setminus B_\epsilon(x)$. An application of the divergence theorem shows that

$$\int_{\partial D_\epsilon} u(\xi) \partial_{\nu_\xi} N(x, \xi) dS_\xi = \int_{\partial D_\epsilon} \partial_{\nu_\xi}^i u(\xi) N(x, \xi) dS_\xi.$$

As ϵ tends to zero this becomes

$$\begin{aligned} \int_{\partial D} u(\xi) \partial_{\nu_\xi} N(x, \xi) dS_\xi + \frac{1}{2} u(x) &= \int_{\partial D} \partial_{\nu_\xi}^i u(\xi) N(x, \xi) dS_\xi \\ &= \frac{1}{k} \int_{\partial D} \partial_{\nu_\xi}^\epsilon u(\xi) N(x, \xi) dS_\xi \end{aligned}$$

or

$$\int_{\partial D} \partial_{\nu_\xi}^\epsilon u(\xi) N(x, \xi) dS_\xi = \frac{k}{2} u(x) + k \int_{\partial D} u(\xi) \partial_{\nu_\xi} N(x, \xi) dS_\xi.$$

This equation, upon substitution into (3.4), yields equation (3.2). \square

Proof of lemma 3.1: From equation (3.2) it follows that

$$\sup_{x \in \partial D} |u(k, x)| \leq \frac{2|1-k|}{1+k} \left(\sup_{\xi \in \partial D} |u(k, \xi)| \right) \left(\sup_{x \in \partial D} \|\partial_{\nu_\xi} N\|_{L^1_\xi(\partial D)} \right) + \frac{2}{1+k} \sup_{\partial D} |u_0|$$

or, with a little rearrangement,

$$\sup_{x \in \partial D} |u(k, x)| \leq \frac{2 \sup_{\partial D} |u_0|}{1+k - 2(1-k) \sup_x \|\partial_{\nu_\xi} N(x, \xi)\|_{L^1_\xi(\partial D)}}.$$

Since $\sup_{x \in \partial D} \|\partial_{\nu_\xi} N(x, \xi)\|_{L^1_\xi(\partial D)}$ is finite ($\partial_{\nu_\xi} N(x, \xi)$ is actually continuous as a function of x and ξ —see [4], section 3C), $\sup_{\partial D} |u|$ is bounded as a function of k for k in some neighborhood of one. In fact, rewriting equation (3.2) as

$$u(k, x) - u_0(x) = \frac{2(1-k)}{1+k} \int_{\partial D} u(\xi) \partial_{\nu_\xi} N(x, \xi) dS_\xi + \frac{1-k}{1+k} u_0(x)$$

and using the boundedness of u as a function of k shows that

$$\sup_{x \in \partial D} |u(k, x) - u_0(x)| \leq C|k-1|.$$

The constant C will depend on D and u_0 . From equation (3.1) and the definition of $\psi(x)$,

$$u(k, x) - u_0(x) - (k - 1)\psi(x) = (1 - k) \int_{\partial D} (u - u_0)(\xi) \partial_{\nu_\xi} N(x, \xi) dS_\xi \quad (3.5)$$

for $x \in \partial\Omega$. Since $\sup_{\partial D} |u - u_0| \leq C|k - 1|$ on ∂D , equation (3.5) shows

$$\sup_{x \in \partial\Omega} |u(k, x) - \tilde{u}(x)| \leq \tilde{C}|k - 1|^2$$

for $x \in \partial\Omega$ and some \tilde{C} , independent of x . This proves Lemma 3.1. \square

Define the linearized solution $\tilde{u}(x)$ as

$$\tilde{u}(x) = u_0(x) + (k - 1)\psi(x).$$

Next we make some restrictions on the map $q \rightarrow D(q)$. First, we require that $D(q) \subset \Omega'$ for some fixed $\Omega' \subset \subset \Omega$ and that the boundary of $D(q)$ is a simple closed curve. Parameterize $\partial D(q)$ as $x = x_q(t), y = y_q(t)$, $0 \leq t \leq 2\pi$ with

$$ds = \sqrt{\left(\frac{dx_q}{dt}\right)^2 + \left(\frac{dy_q}{dt}\right)^2} \equiv \frac{L}{2\pi} \quad (3.6)$$

where L is the length of the boundary of D . We also require that for all $q \in Q$,

$$\|x_q\|_{C^2[0, 2\pi]} \leq K$$

$$\|y_q\|_{C^2[0, 2\pi]} \leq K$$

for some constant K . This follows, for example, if the curvature of $\partial D(q)$ is bounded. Finally, we require that if $q \rightarrow q_0$ in \mathbb{R}^m then $D(q) \rightarrow D(q_0)$,

where convergence of these domains means that for each $\epsilon > 0$ there is a number $\delta > 0$ so that

$$\begin{aligned}\|x_q - x_{q_0}\|_{C^2[0,2\pi]} &\leq \epsilon, \\ \|y_q - y_{q_0}\|_{C^2[0,2\pi]} &\leq \epsilon\end{aligned}$$

whenever $|q - q_0| \leq \delta$ (δ is independent of q_0).

We now reformulate the original inverse problem, using the linearized solution \tilde{u} in place of u :

$$(IDP) \quad \text{minimize } J(q) \text{ for } q \in Q$$

where $J(q)$ is defined as

$$J(q) = \frac{1}{2} \sum_{i=1}^M |y_i^q - d_i|^2,$$

but with $y^q = \mathcal{F}(\tilde{u}^q)$, where \tilde{u}^q is the linearization of the solution to (1.1) with $D = D(q)$ and \mathcal{F} and the d_i are as defined in the introduction.

One can prove that the problem (IDP) has a solution. The conditions on the map $q \rightarrow D(q)$ guarantee the continuity of the map

$$q \rightarrow u_0(x) + (k-1) \int_{\partial D} u_0(\xi) \partial_{\nu_\xi} N(x, \xi) dS_\xi$$

as a map from \mathbb{R}^m to $L^2(\partial\Omega)$ ($\partial_{\nu_\xi} N(x, \xi)$ is smooth for $x \in \partial\Omega$ and $\xi \in \partial D$), provided the Neumann data g is regular enough, for example, $g \in L^2(\partial\Omega)$. The map \mathcal{F} is continuous from $L^2(\partial\Omega)$ to \mathbb{R}^M so that $q \rightarrow J(q)$ is continuous and hence $J(q)$ attains a minimum for some $q^* \in Q$. Moreover, the map

$q \rightarrow \tilde{u}$ is differentiable if the map $q \rightarrow (x_q(t), y_q(t))$ is differentiable, so that we may use an optimization scheme involving evaluation of derivatives in solving (IDP).

Remark: If the Neumann data g is not sufficiently regular then the function u_0 may not be in $L^2(\partial\Omega)$; however, suppose that $u_0 \in L^2(S)$ where $S \subset \partial\Omega$. Then the above argument remains valid if we require that the electrode locations N_i be subsets of S . Also, if g is smooth enough on $S \subset \partial\Omega$ then u_0 will be continuous on S . In this case we may take the functions f_i to be δ_{p_i} , delta functions at points $p_i \in N_i$, so that \mathcal{F} is simply a point-by-point sample. The proofs above and in section 4 remain essentially unchanged.

4 A computational method

In this section we will consider a computational method for solving the identification problem (IDP). An n point quadrature rule η_n on the interval $[0, L]$ is a set of pairs of real numbers $\{t_i, \omega_i\}$, $t_i \in [0, L]$, for $i = 1, \dots, n$. We will say that the family of quadrature rules $\{\eta_n\} = \{t_{in}, \omega_{in}\}$, $i = 1, \dots, n$, is convergent if for any $\phi \in C^1[0, L]$,

$$\left| \sum_{i=1}^n \omega_{in} \phi(t_{in}) - \int_0^L \phi(t) dt \right| \rightarrow 0 \quad (4.1)$$

as $n \rightarrow \infty$. The convergence of the family $\{\eta_n\}$ will be called uniform if the convergence in (4.1) is uniform over the set $\{\phi \in C^1[0, L]; \|\phi\|_{C^1[0, L]} \leq A\}$ for any constant A , i.e., the rate of convergence depends only on C^1 bounds for ϕ .

Given a quadrature rule $\eta_n = \{t_{in}, \omega_{in}\}$ define $J^n(q)$ as

$$J^n(q) = \frac{1}{2} \sum_{i=1}^M |\tilde{y}_i^q - d_i|^2,$$

with $\tilde{y}^q = \mathcal{F}(\tilde{u}_n^q)$, \mathcal{F} and d_i as previously defined and \tilde{u}_n^q defined by

$$\tilde{u}_n^q(x) = u_0(x) + (k-1) \frac{L}{2\pi} \sum_{i=1}^n \omega_{in} u_0(\xi(t_{in})) \partial_{\nu_\xi} N(x, \xi(t_{in}))$$

where $\xi(t)$ is a parameterization of $\partial D(q)$ satisfying (3.6). Define the discrete approximation to the identification problem (IDP):

$$(AIDP)^n \quad \text{minimize } J^n(q) \text{ for } q \in Q.$$

Theorem 4.1 *Let $\{\eta_n\}$ be a uniformly convergent family of quadrature rules and let q^n be the solution to the associated problem $(AIDP)^n$. Then the sequence q^n contains a subsequence q^{n_m} converging to some $q^* \in Q$. Moreover, q^* is a solution to (IDP).*

Proof: If $D = D(q)$ for some $q \in Q$ and ∂D is parameterized in (ξ_1, ξ_2) coordinates as $\xi(t) = (\xi_1(t), \xi_2(t))$, subject to the condition (3.6) then, written out in terms of the parameterization,

$$\psi(x) = \int_0^{2\pi} u_0(\xi(t)) \nabla_\xi N(x, \xi(t)) \cdot \frac{d\xi}{dt} dt \quad (4.2)$$

for $x \in \partial\Omega$. Since N and its derivatives are continuous as functions of x and ξ for $x \in \partial\Omega$ and $\xi \in \Omega'$, we can bound them uniformly for x and ξ in these sets. Similarly u_0 and its derivatives are bounded on Ω' . Using these facts,

as well as $D(q) \subset \Omega'$ for all $q \in Q$, one can bound the integrand and its first derivative (as functions of t), uniformly for $q \in Q$ and $x \in \partial\Omega$. It follows that

$$\sum_{i=1}^n \omega_{in} u_0(\xi(t_{in})) \nabla_{\xi} N(x, \xi(t_{in})) \cdot \frac{d\xi}{dt}(t_{in}) \rightarrow \psi(x)$$

as $n \rightarrow \infty$, uniformly for $q \in Q$, $x \in \partial\Omega$, so that $\tilde{u}_n^q(x) \rightarrow \tilde{u}^q(x)$. The operator \mathcal{F} is continuous from $L^2(\partial\Omega)$ to \mathbb{R}^M so that $J^n(q) \rightarrow J(q)$ uniformly with respect to q . Hence if q^m is a sequence in Q with $q^m \rightarrow q$ then

$$\lim_{m,n \rightarrow \infty} J^n(q^m) = J(q). \quad (4.3)$$

Let q^n be a solution to (AIDP) n . Since Q is compact some subsequence q^{n^m} converges to $q^* \in Q$. For any $q \in Q$ we have

$$J^n(q^n) \leq J^n(q).$$

Taking the limit over n and using (4.3) shows that

$$J(q^*) \leq J(q)$$

so q^* solves (IDP). \square

5 Numerical Results

We will begin with a simple case. As mentioned, Ω will be taken to be the unit disk in \mathbb{R}^2 . The family of subdomains $D(q)$ will consist of disks centered at (a, b) with radius r , so that $q = (a, b, r)$. The set Q will consists of those points satisfying $\sqrt{a^2 + b^2} + r \leq \rho < 1$, so that each domain is contained

in Ω and is bounded away from $\partial\Omega$. It is straightforward to verify that this family satisfies the conditions stated in section 3. Moreover, we can directly compute the derivatives of \tilde{u} with respect to a , b , and r .

For the applied current flux we take $g = -\pi\partial_\tau\delta_\omega$ where ∂_τ is the counter-clockwise tangential derivative and δ_ω is the dirac delta function at $\omega \in \partial\Omega$. The harmonic function u_0 with this Neumann data is known in closed form and for $\omega = (1, 0)$ is given in (x, y) coordinates by

$$u_0(x, y) = \frac{y}{(1-x)^2 + y^2}.$$

Note that this function is not L^2 on $\partial\Omega$, but is smooth and bounded away from the point $(1, 0)$ (see remarks at the end of section 3). The electrode locations will be taken as $p_i = (\cos(2\pi i/16), \sin(2\pi i/16))$ for $i = 1, \dots, 15$ and for the functions f_i we simply set $f_i = \delta_{p_i}$, so $\mathcal{F}(u)$ is just a point-by-point sample of u at the points p_i .

A 10-point Gauss-Legendre integration rule was used to approximate $\psi(x)$ and so obtain the discrete approximation $\tilde{J}(q)$ to $J(q)$. The derivatives of $\tilde{J}(q)$ were computed by simply differentiating the sum $\tilde{J}(q)$ with respect to q . The function $\tilde{J}(q)$ was minimized using a Levenberg-Marquardt optimization procedure with initial guess $q = (0, 0, 0.1)$. The simulated data for the linearized inverse problem was generated by evaluating $\tilde{u}(x)$ at the points $x = p_i$. To simulate noise in the data, independent gaussian random variables were added at noise levels of 0%, 5%, 10% and 20%, e.g., for 10% noise the random variables added had a mean square value of $0.1 \times \|u - u_0\|_{L^2(\partial\Omega)}^2$ in the data. The results are summarized in table 1. The value of k was chosen as 1.1, although for the linearized problem the value of k is irrelevant.

Figure 1 shows the accuracy of the the linearized solution as an approximation to the true solution for $k = 1.1$ and $k = 2.0$, the region D being that used for figures 3 through 7. The graphs are of $u - u_0$ and $\tilde{u} - u_0$. The forward problem was solved by using Nyström's method (see [1]) on the Fredholm equation (3.2) to solve for u on ∂D and then representing u on the boundary of Ω by means of equation (3.1). Tables 2 and 3 summarize the results when the optimization is applied using data from the full non-linear forward problem. Here the value of k is relevant; the algorithm should perform best for k near 1. The tables present results for $k = 1.1$, and $k = 0.5$.

To apply this method to more general regions we need a way to describe D using finitely many parameters. We'll assume $\partial D(q)$ can be described as

$$\begin{aligned}x(t) &= a + r(t) \cos(t) \\y(t) &= b + r(t) \sin(t)\end{aligned}$$

for $0 \leq t \leq 2\pi$, where a and b are constants and $r(t)$ is a C^2 cubic spline satisfying $r(t_i) = q_i$, $i = 1, \dots, m$ with $t_i = 2\pi i/m$ with the endpoint conditions $r(0) = r(2\pi)$ and $r'(0) = r'(2\pi)$. It can be verified that the conditions (3.6) are satisfied provided the q_i are bounded away from zero. This algorithm was implemented as follows. First, apply the algorithm which assumes D is a disk to recover that disk centered at (a, b) with radius r which best fits the boundary data. Second, with this choice for a and b and the initial guess $q_i = r$ apply the optimization procedure (Levenberg-Marquardt) in the variables q_1, \dots, q_m . A smooth penalty term, identically zero for $q_i \geq 0.01$, was added to $\tilde{J}(q)$ to ensure that the q_i were bounded away from zero. This

term was of the form $\sum_{i=1}^5 (f(x))^2$ with f taken to be

$$f(x) = \begin{cases} c_3(x - c_1)^2 \exp -c_2/(x - c_1)^2 & x < c_1 \\ 0 & x \geq c_1 \end{cases}$$

for constants $c_1 = 0.01$, $c_2 = 3.05e - 5$, $c_3 = 1.36e4$.

In Figures 3 through 8, $m = 5$, $a = 0.2$, $b = 0.4$, $q_1 = q_2 = 0.032$, $q_3 = 0.056$, and $q_4 = q_5 = 0.04$, respectively. The linearized forward problem was solved (with a dipole at $(1,0)$) and the optimization procedure applied to the resulting data. Figure 3 shows the region $D(q)$ and the best fit disk. Figure 4 shows the region recovered by optimizing over q with (a, b) fixed as the center of the best fit disk. Figure 5 shows the region $D(q)$ and recovered estimate when 10% noise is added to the data.

The optimization procedure for the linearized problem was also applied to data generated by solving the full non-linear forward problem. The region $D(q)$ is chosen as in the previous example. Figure 6 shows the recovered estimate of $D(q)$ when $k = 1.1$, using a single dipole at $(1,0)$. Figure 7 shows the same with $k = 0.5$ and figure 8 with $k = 3.0$. For k near one the estimate of D is good. For values of k farther from one the estimates of D are correct in location and approximate size, but the details of the shape are lost.

Finally, one is not restricted to using a single applied current flux. An obvious extension of the previous results allows one to apply the linearized approximation for multiple current fluxes. The functional $\tilde{J}(q)$ is then simply defined as the sum of the $\tilde{J}_i(q)$ where $\tilde{J}_i(q)$ is the cost functional for the i th current flux. For Figure 9 the region $D(q)$ was chosen to be a disk

centered at $(0.3, -0.3)$ with radius 0.05 and $k = 1.5$. In the first figure a single dipole current was applied and 50% noise added to the data from the forward problem. In the second figure 8 dipole currents were applied, the dipoles located at $(\cos(\pi i/4), \sin(\pi i/4))$, $i = 0, \dots, 7$, again with 50% noise added.

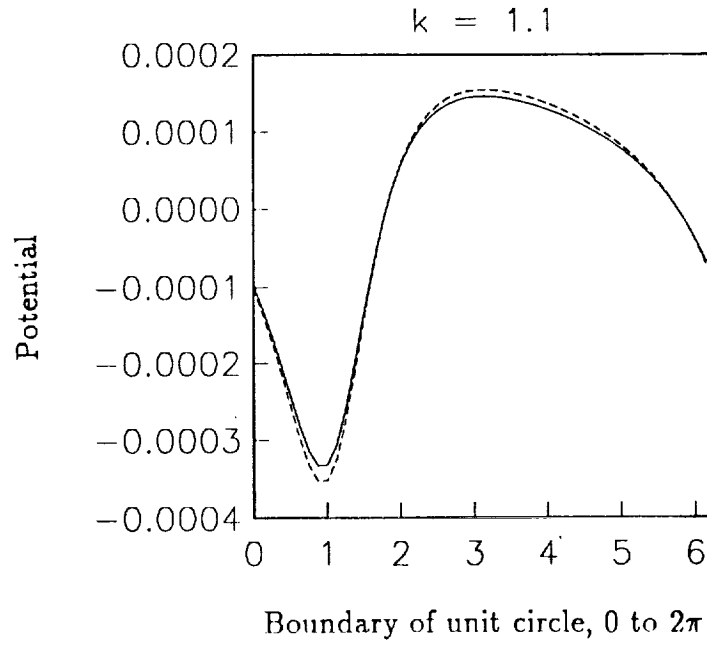


Figure 1: Function $u - u_0$ (solid line) and $\tilde{u} - u_0$ (dashed line) for $k = 1.1$.

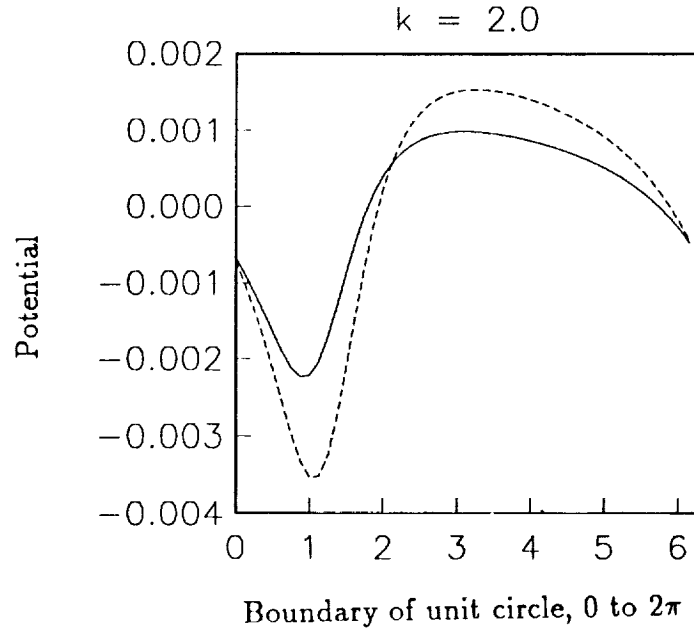


Figure 2: Function $u - u_0$ (solid line) and $\tilde{u} - u_0$ (dashed line) for $k = 2.0$.

q	true	Noise free	5% noise	10% noise	20% noise
a	0.2	0.2000	0.2010	0.2026	0.2639
b	0.3	0.3000	0.2952	0.2891	0.2945
r	0.05	0.0500	0.0507	0.0491	0.0452
iterations		5	5	6	6
$J(q)$		5.67×10^{-19}	1.27×10^{-9}	5.46×10^{-9}	6.94×10^{-8}

Table 1: Summary of results for linearized inverse problem

q	true	Noise free	5% noise	10% noise	20% noise
a	0.2	0.1999	0.2028	0.2258	0.1582
b	0.3	0.3000	0.2987	0.2899	0.3144
r	0.05	0.0512	0.0506	0.0503	0.0550
iterations		5	5	6	6
$J(q)$		7.28×10^{-19}	2.50×10^{-9}	7.96×10^{-9}	2.46×10^{-8}

Table 2: Summary of results for full non-linear problem, $k = 1.1$.

q	true	Noise free	5% noise	10% noise	20% noise
a	0.2	0.1991	0.2090	0.1722	0.2170
b	0.3	0.3003	0.3015	0.3293	0.2927
r	0.05	0.0578	0.0575	0.0604	0.0551
iterations		5	5	5	5
$J(q)$		3.54×10^{-17}	1.41×10^{-7}	3.40×10^{-7}	8.74×10^{-7}

Table 3: Summary of results for full non-linear problem, $k = 0.5$.

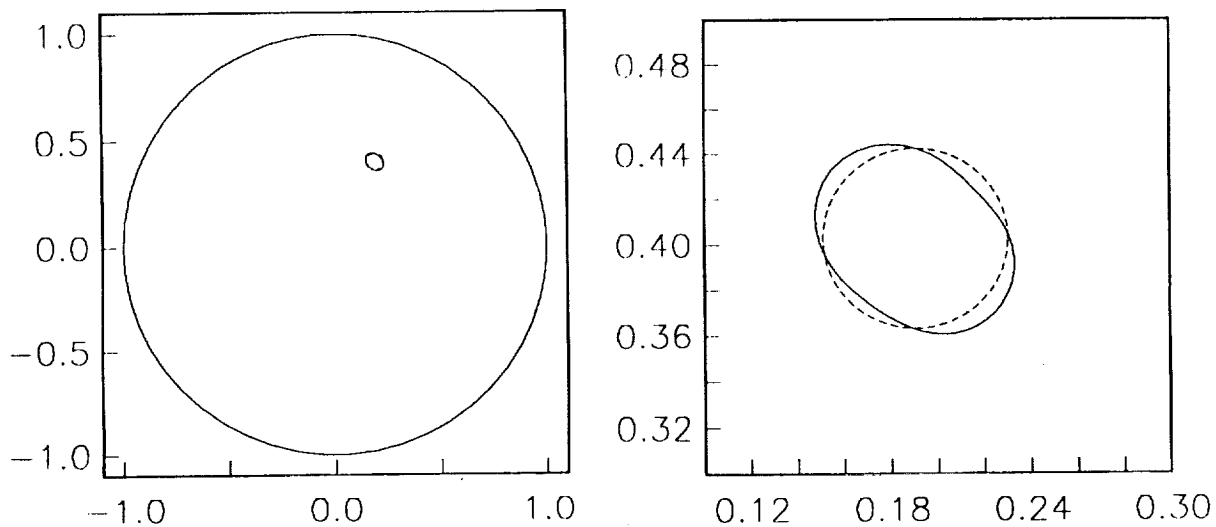


Figure 3: Two views of actual region D (solid line) and best fit disk (dashed line).

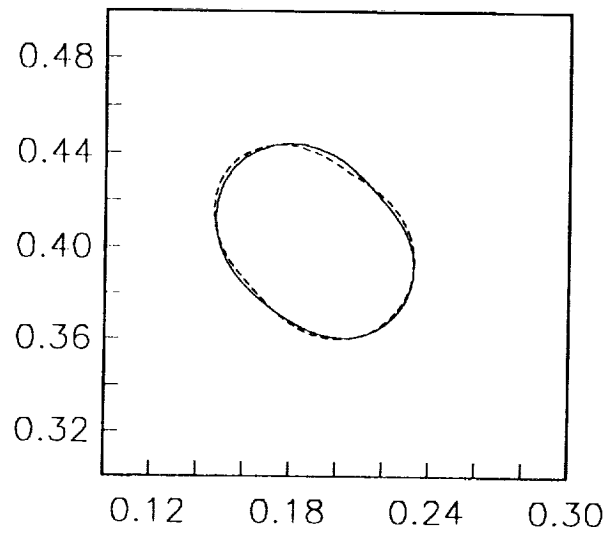


Figure 4: Actual region D (solid line) and recovered estimate (dashed line).

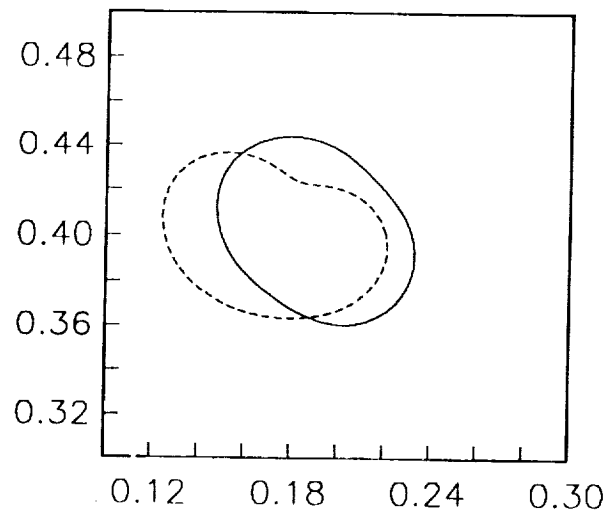


Figure 5: Actual region D (solid line) and recovered estimate (dashed line) with 10% noise added to input data.

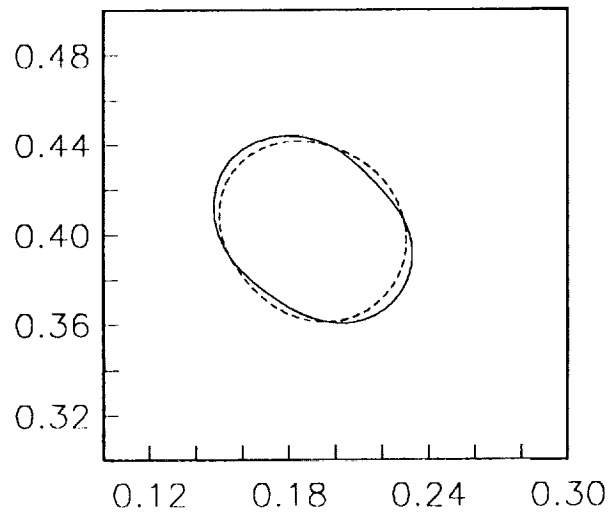


Figure 6: Actual region D (solid line) and recovered estimate (dashed line),
 $k = 1.1$.

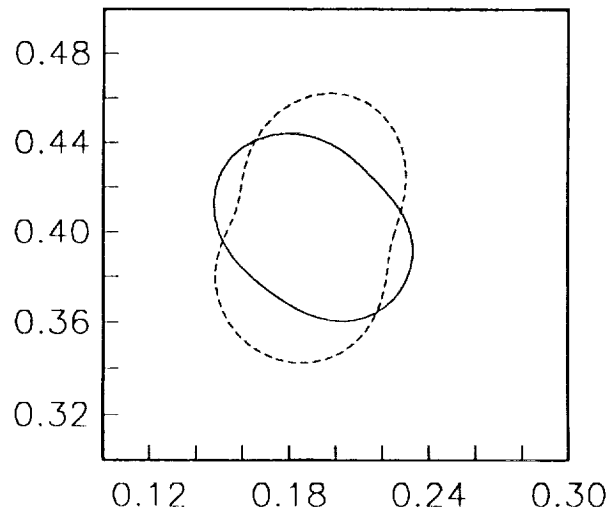


Figure 7: Actual region D (solid line) and recovered estimate (dashed line),
 $k = 0.5$.

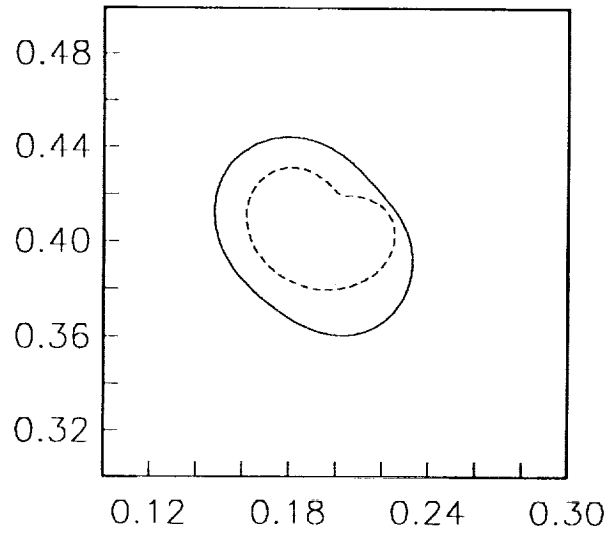


Figure 8: Actual region D (solid line) and recovered estimate (dashed line),

$k = 3.0$.

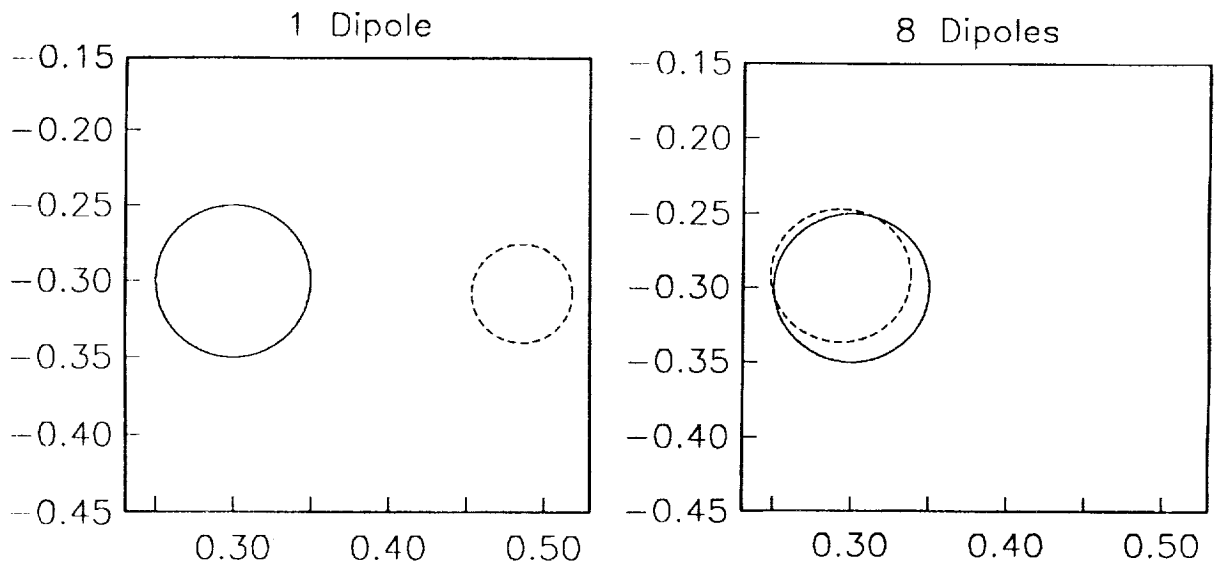


Figure 9: Actual region D (solid line) and recovered estimate (dashed line),

$k = 1.5$, using 1 and 8 applied dipole currents, respectively.

References

- [1] Atkinson, K.E., *A survey of numerical methods for the solution of fredholm integral equations of the second kind*, SIAM, Philadelphia, PA, 1976.
- [2] Barber D.C and B.H. Brown, *Recent developments in applied potential tomography-APT* Information Processing in Medical Imaging, ed. S.I. Bacharach, 106-121. Nijhoff, 1986.
- [3] Bellout, H. and Friedman, A. *Identification problems in potential theory*, Arch. Rat. Mech. Anal. 101 (2), 1988, 143-160.
- [4] Folland, Gerald B., *Introduction to partial differential equations*. Princeton, NJ: Princeton University Press, 1976.
- [5] Friedman, A., *Detection of mines by electric measurements*, Siam J. Appl. Math 47, 1987, pp.201-212.
- [6] Gilbarg, D. and Trudinger, N.S., *Elliptic partial differential equations of second order*. New York: Springer-Verlag, 1983.
- [7] Isakov, V., *On uniqueness of recovery of a discontinuous conductivity coefficient*, Comm. Pure Appl. Math, 41 (1988), 865-877.
- [8] Kohn, R., and Vogelius, M., *Determining conductivity by boundary measurements II. Interior results*, Comm. Pure Appl. Math, 38 (1985), 643-667.

- [9] Ladyzhenskaya, O.A. and N.N Ural'tseva, *Linear and quasilinear elliptic equations*. New York: Academic Press, 1968.



Report Documentation Page

1. Report No. NASA CR-187543 ICASE Report No. 91-33		2. Government Accession No.		3. Recipient's Catalog No.	
4. Title and Subtitle NUMERICAL RECOVERY OF CERTAIN DISCONTINUOUS ELECTRICAL CONDUCTIVITIES				5. Report Date March 1991	
				6. Performing Organization Code	
7. Author(s) Kurt Bryan				8. Performing Organization Report No. 91-33	
				10. Work Unit No. 505-90-52-01	
9. Performing Organization Name and Address Institute for Computer Applications in Science and Engineering Mail Stop 132C, NASA Langley Research Center Hampton, VA 23665-5225				11. Contract or Grant No. NAS1-18605	
				13. Type of Report and Period Covered Contractor Report	
12. Sponsoring Agency Name and Address National Aeronautics and Space Administration Langley Research Center Hampton, VA 23665-5225				14. Sponsoring Agency Code	
15. Supplementary Notes Langley Technical Monitor: Michael F. Card Submitted to Inverse Problems Final Report					
16. Abstract <p>The inverse problem of recovering an electrical conductivity of the form $\gamma(x) = 1 + (k-1)\chi_D$ (χ_D is the characteristic function of D) on a region $\Omega \subset \mathbb{R}^2$ from boundary data is considered, where $D \subset \subset \Omega$ and k is some positive constant. A linearization of the forward problem is formed and used in a least squares output method for approximately solving the inverse problem. Convergence results are proved and some numerical results presented.</p>					
17. Key Words (Suggested by Author(s)) inverse problem, impedance tomography, domain identification				18. Distribution Statement 64 - Numerical Analysis Unclassified - Unlimited	
19. Security Classif. (of this report) Unclassified		20. Security Classif. (of this page) Unclassified		21. No. of pages 28	22. Price A03

